Indian Journal of Engineering & Materials Sciences
Vol. 29, February 2022, pp. 124-129

Evaluation of pharmacological and catalytic activity of CuO and Zn doped CuO nanoparticles

R Saranya[a], M Mubarak Ali[b]*, & K Jeyalakshmi[c]

[a]Centre for Research and Evaluation, Department of Chemistry, Bharathiar University, Coimbatore 641 046, Tamil Nadu, India

[b]Department of Chemistry, Chikkaiah Naicker College, Erode, Tamil Nadu 638 004, India

[c]Department of Chemistry, M Kumarasamy College of Engineering, Karur, Tamil Nadu 639 113, India

Received: 3 January 2021 ; Accepted: 10 August 2021

CuO and Zn doped CuO nanoparticles (Zn-CuO NPs) with varying concentration i.e., $Zn_xCu_{1-x}O$ (where x = 0, 0.5, 1, and 1.5%) have been prepared via microwave assisted method. The spheroid structure of CuO NPs and the nanorod structure of Zn-CuO NPs have been determined using High Resolution Scanning Electron Microscopy (HR-SEM) analysis. Elemental analysis has been carried out using Energy Dispersive X-ray Analysis (EDAX). The particle size and surface area of CuO and Zn-CuO NPs have been confirmed by Brunauer–Emmett–Teller (BET) method. The antibacterial studies have been revealed that $Zn_{(1.5\%)}$-CuO NPs exhibited maximum zone of inhibition (19-29 mm) against the tested four bacterial strains. Zn-CuO NPs have been displayed robust action of antibacterial activity with minimum inhibitory concentration (MIC) of 0.09 µM against *Campylobacter coli* (*C. Coli*). DPPH and H_2O_2 radical scavenging assay investigation have been revealed that the significant scavenging activity has showed by $Zn_{(1.5\%)}$-CuO. The *in vitro* cytotoxicity evaluation of synthesized material against human breast (MCF7) and human lung (A549) cancer cell lines have been demonstrated that $Zn_{(1.5\%)}$-CuO NPs exhibited better cytotoxic activity against MCF7 cell lines (97.5% cell death) than A549 cell lines (90% cell death).

Keywords: CuO, Zn-CuO NPs, Antibacterial, Antioxidant, Cytotoxicity, MCF7, A549

1 Introduction

CuO NPs have been extensively exploited due to their natural abundance, cost effective and eco-friendly nature. It has been finded applications in the field of catalysis, conductivity, water treatment, textile industries, agricultural practices and pharmaceutical activities[1-6]. Due to its importance, various synthesis routes have been adopted for CuO nanostructures such as sol-gel[7], hydrothermal[8], solvothermal[9], electro-deposition[10] and co-precipitation[11] etc. When it has been compared to the above conventional methods microwave assisted method is very easy and ecofriendly to synthesis the nano materials[12]. Microwave assisted method enhances the rate of the reaction and provides better yield with energy economy. In this work greener synthesis has been achieved by microwave method. Moreover, there are numerous reports on the fabrication of CuO nanomaterials with various types of dopant which have significant antibacterial activity. These fabricated nanomaterials have been proposed for the applications in medical wears[13-15].

It has been reported that the physio-chemical behavior of CuO nanomaterials can be customized via doping[16]. Dopant has been playing an important role in altering the structural and electrical properties of the metal monoxides. Many researchers have been reported the changes made with the doping of transition metals such as Mn, Ni, Fe, Ti, Cd and Zn into CuO lattice[17, 18]. Among these, Zn^{2+} dopant is the promising because of its similar ionic radii (0.074 nm) to that of Cu^{2+} (0.072 nm) and possesses similar ionic states. This renders higher thermodynamic solubility of Zn in CuO host matrix. Furthermore, it has been reported that Zn^{2+} dopant can effectively produce defects in CuO nanostructures which may be potential for biological and catalytic applications[19, 20].

There are huge reports on Zn doped CuO NPs have been exhibiting enhanced deterioration of *Staphylococcus aureus* (S. aureus) and *Escherichia coli* (E. coli) in both regular and multidrug resistant bacteria compared to ZnO NPs and CuO NPs[21]. Zn-CuO NPs have been exhibited potent anti-tumor effect on pancreatic cancer both *in vitro* and *in vivo*[22]. The excellent properties of CuO such as oxidative stress, cell cycle arrest, apoptosis and antioxidative exhaustion against the cancer cells have been induced by Zn doping to lead to the cancer cells death in the kidney cancer therapy[23]. There were also having

*Corresponding author (E-mail: masterscience2003@yahoo.co.in)

reports to support that the catalytic activity was also enhanced by doping of Zn to CuO[24]. The goal of the contemporary effort is to synthesis CuO and Zn-CuO NPs by microwave assisted method. The synthesized nanoparticles have been evaluated for its catalytic, antibacterial, antioxidant and cytotoxic activities.

2 Materials and Methods

2.1 Preparation of pure and Zn-doped cuo

All the materials used were of analytical grade obtained from Merck, India and used without further purification. Pure and Zn-CuO NPs were synthesized by microwave combustion method using the precursors and urea as a fuel. Zn-CuO NPs were synthesized by treating 0.5, 1.0, and 1.5 weight percentages of zinc nitrate and copper nitrate dihydrate solutions and stirred for 25 minutes. These solutions were mixed for 1 h at room temperature (32± 1°C) and 1.1 mL of thioglycolic acid (TGA) was mixed slowly with constant stirring for 15 minutes to obtain clear transparent solution. It was then placed in microwave-oven (2.45 GHz, 850 W) for 10 minutes. The obtained samples were thoroughly washed with alcohol for several times and the final product was then dried in a hot air oven at 80 °C for 2 h. Pure CuO was synthesized following the same procedure mentioned above without the addition of zinc nitrate.

2.2 Characterization

The structure and crystallite size of pure and Zn-CuO NPs was determined using a Philips X'pert (Germany) X-ray diffractometer with Cu-K_α radiation at λ = 1.5418 Å. The average crystallite size was calculated by measuring the full width at the half maximum (FWHM) by using Debye-Scherrer equation[25]. The structural assignments were made with reference to the JCPDS powder diffraction files. Morphological observations along with the chemical composition have been performed using Jeol JSM6360 (Japan) HR-SEM equipped with EDAX. The alterations in surface area and particles were examined via nitrogen adsorption analysis (BET) on a Micrometrics ASAP 2020 apparatus (USA). The samples were degassed at 200 °C for 20 minutes under 0 to 950 mm Hg pressure before doing the experiments[26].

2.3 Catalytic tests

To investigate the catalytic activity of Zn-CuO NPs, the oxidation reaction of benzyl alcohol was carried out. The reaction condition, particularly the concentration of the material was varied from 55 to 85%. The conversion and selectivity (%) were calculated. The mixture of oxidant (H_2O_2) and solvent (acetonitrile) were heated at 80 °C in basic medium for 8 h in a three necked round bottom flask equipped with a reflux condenser with thermometer. The product of the catalytic reaction was analyzed by Agilent GC spectrometer (USA). The column used for this analysis was DB wax column (capillary column) of length 30 mm and helium was used as the carrier gas.

2.4 Antibacterial tests

To investigate the antibacterial efficacy of the synthesized material, the concentration of CuO and Zn-CuO NPs was adjusted to 0.1 g/L, with the concentration of bacterial solution kept constant [10^7 colony-forming unit (CFU) mL^{-1}]. After 5, 10, 20, 30 minutes, 0.2 mL of supernatant liquid was extracted and streaked onto well solidified agar nutrient plates. After 24 h incubation at 37 °C, the colonies were measured. The bacterial strains were inoculated separately in 30 mL of nutrient broth in a conical flask and incubated for 24 h to get active strain by using well diffusion method. Muller Hinton agar was poured separately into petri dishes. After the medium solidified, a well was made in the plates with sterile borer (5mm). About 40 µL of the test sample was introduced into the well and the plates were incubated at 37 °C for 72 h. All samples were tested in triplicates. The minimum inhibitory concentration (MIC) was determined.

2.5 Antioxidant activity

Antioxidant activity of CuO and Zn-CuO NPs along with standard has been examined with reference to DPPH and H_2O_2 radical scavenging assays[27-30]. The colloidal suspensions of Zn were sonicated at room temperature for 30 minutes to avoid nanoparticles agglomeration. The absorbance was measured spectrophotometrically against the corresponding blank solutions[31]. The procedure involved in the scavenging assay is given in the supplementary information.

2.6 Cell line and culture

MCF7 and A459 cell lines were maintained in 10% FBS, penicillin (100 U/mL) and streptomycin (100 µg/mL) in a humidified atmosphere of 50 µg/mL of CO_2 at 37 °C. The cell lines were grown in Eagle's minimum which contains 10% fetal bovine serum (FBS). 100 µL per well of cell suspension were

seeded into 96-well plates at plating density of 10,000 cells/well and incubated. After 24 h the cells were treated with serial concentrations of the test samples which were dissolved in DMSO. Triplication was maintained and the medium without the test sample served as the control. After 24 h, the wells were treated with 20 µL MTT [5 mg mL^{-1} Phosphate Buffered Saline (PBS)] and incubated at 37 °C for 4 h. The medium with MTT was then removed separately and the formed formazan crystals were dissolved in 100 mL DMSO. The absorbance at 570 nm was measured using an ELISA plate reader. The graph was plotted between the percentage of cell death and the concentration of the CuO and Zn-CuO NPs.

3 Results and Discussion

3.1 Powder X-ray Diffraction (XRD) analysis

The characteristics X-ray diffraction patterns of pure and Zn-CuO NPs were recorded in the range of 2θ between 20º-80º shown in Fig. 1. The obtained XRD diffraction peaks for pure and Zn-CuO NPs were located at 2θ = 31.0, 37.0, 44.5, 56.0, 59.5 and 65.5. These peaks can be assigned to the preferred orientation of (111), (200), (211), (221), (310) and (222) of the monoclinic structure of pure and Zn-CuO NPs. The diffraction peaks of the material agreed well with the diffraction data from the JCPDS file number (06-2151).

The peaks indicated that Zn ions were successfully doped into the lattice of Cu sites without affecting the crystal structure of the parent CuO. The atomic radius of Cu^{2+} ion (0.73 Å) and Zn^{2+} (0.74 Å) are almost similar. Hence, Cu^{2+} ions in the lattice structure can be well replaced by Zn^{2+} ions. Intensity of XRD peaks of Zn-CuO NPs sample was found to reduce in comparison to that of pure CuO which indicates a decrease in crystallinity of CuO NPs with Zn doping. The wider and lowered peaks obtained for Zn-CuO was due to the occurrence of lattice strain on increasing Zn concentration in CuO matrix[32]. The very slight shift in peak positions were observed with Zn-CuO indicating that the all doped material occupied the substitution sites[33, 34].The average crystallite size of CuO and Zn-CuO ($Zn_{0.5\%}$, $Zn_{1.0\%}$, $Zn_{1.5\%}$) was 30.43, 26.65, 23.76 and 19.24 nm respectively.

3.2 SEM and EDAX studies

Figures 2(a-d) depicts the FESEM micrographs of CuO (a) and Zn-CuO (b-d) NPs which clearly showed the irregular shaped morphologies of the material. On the other hand, it showed that the shape of the doped particles changed from spheroid to rod-like structure. The images indicated that the concentration of Zn affects the morphology of pure CuO. The slight differences in particle size values were observed which may be due to the molecular structural disorder, lattice strain and clustering of the nanostructures[35].

Fig. 2 depicted the rod-like shape of the synthesized CuO NPs as a function of Zn dopant concentration. The elemental composition of pure CuO and Zn-CuO NPs annealed at 400 °C was obtained from EDAX analysis. Fig. 3 interpreted the EDAX spectra of CuO (a) Zn-CuO NPs (b-d). The EDAX results showed that there were no other elemental impurities present in the material and it indicated the presence of Cu with O and Cu, O with Zn.

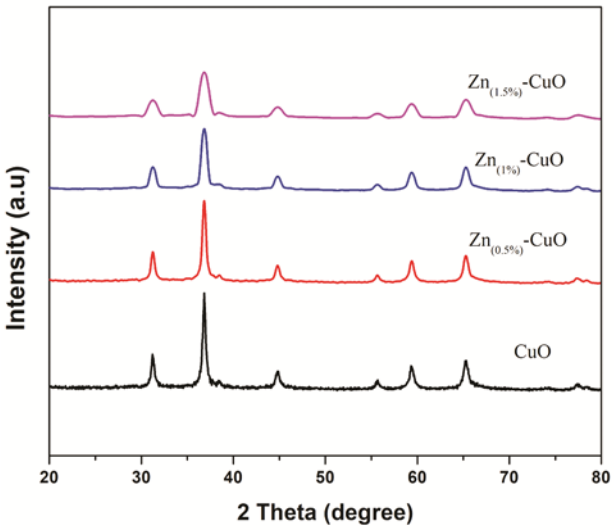

Fig. 1 — XRD pattern of CuO, and Zn-CuO NPs.

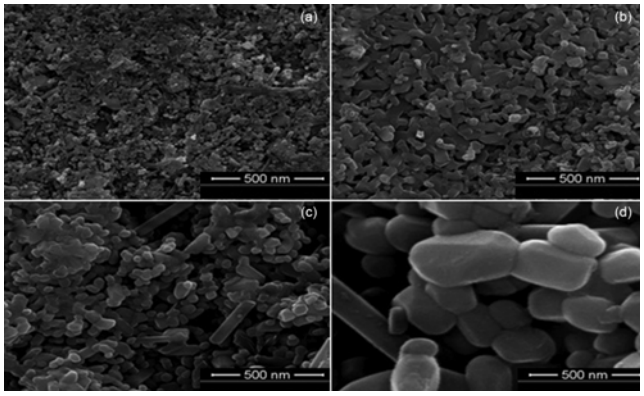

Fig. 2 — SEM image of (a) CuO, (b) $Zn_{(0.5\%)}$-CuO, (c) $Zn_{(1.0\%)}$-CuO, and (d) $Zn_{(1.5\%)}$-CuO.

3.3 Surface area and particle size

The size and shape-dependent properties and the increased surface-to-volume ratio influence the performance of materials[36]. The XRD results showed that size and shape of the Zn-CuO NPs depend on the Cu precursor. The changes in the precursor lead to great effects on the size of Zn-CuO and reaction time of Zn-CuO NPs formation. The chemical reactivity, adsorption, bacterial activity and electrical properties of the nanostructure mainly rely on the surface area[37]. The specific surface area of the prepared nanostructures has been obtained via BET method. Fig. 4 showed that the particle size of the CuO NPs decreased with the increase in the dopant concentration. This influenced the surface area of the Zn-CuO NPs. The particle size of CuO was 30 nm with the surface area of 46 m^2/g but the particle size of Zn doped CuO was found to be 19 nm with increased surface area of 78 m^2/g. The results also clearly indicated that the surface area of Zn doped CuO was higher than that of CuO material.

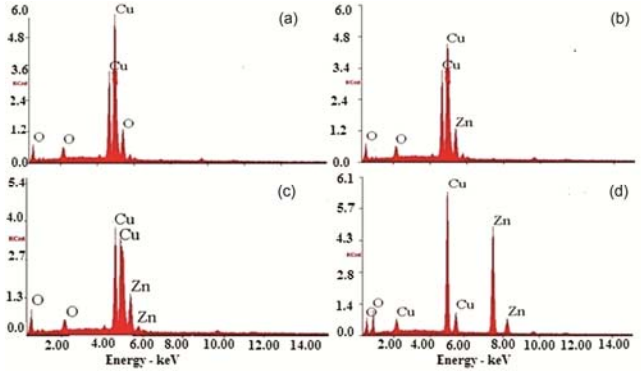

Fig. 3 — EDAX spectra of (a) CuO, (b) $Zn_{(0.5\%)}$-CuO, (c) $Zn_{(1.0\%)}$-CuO, and (d) $Zn_{(1.5\%)}$-CuO.

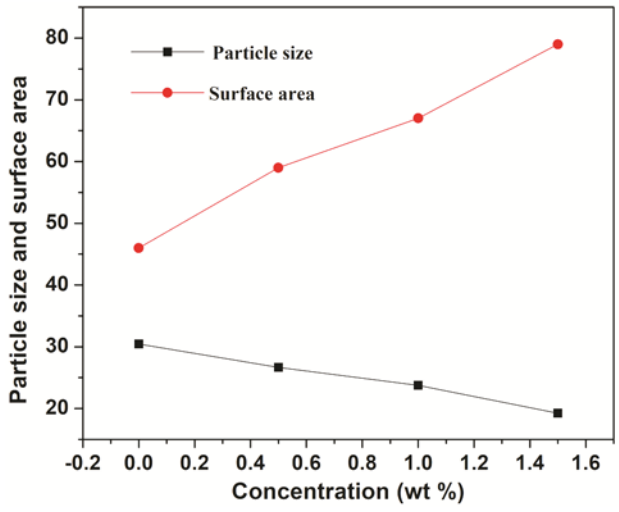

Fig. 4 — Correlation of particle size (nm) and surface area (m^2/g) for CuO, and Zn-CuO NPs.

3.4 Catalytic applications

CuO and Zn-CuO NPs were investigated for its catalytic activity. The catalytic performance of the material was evaluated for the oxidation reaction of benzyl alcohol to benzaldehyde. The catalytic studies showed that the doping has a strong influence on both the conversion and product selectivity (Fig. 5). The influence in the catalytic ability was due to the increase in the surface area of Zn-CuO nanoparticles. Subsequently, Zn-CuO catalyst was able to oxidize benzylalcohol to benzaldehyde in an efficient and ecofriendly manner so that they are promising contenders for the industrial applications[38].

3.5 Antibacterial activity

The results of antibacterial activity of CuO and with various concentrations of Zn-CuO NPs were studied. The zone of inhibition of CuO and Zn-CuO rods were shown in Fig. 6. The antibacterial activity of CuO and Zn-CuO NPs was exploited by mixing with wound dressing materials. The growth behavior of *Staphylococcus aureus* (*S. aureus*), *Bacillus Subtilis (B. subtilis), Klebsiella and Campylobacter coli* (*C.Coli*) bacterial strains in the presence of the prepared CuO and Zn-CuO NPs has been studied via optical density OD growth curve tests[39]. Fig. 6 represented the growth curvatures of *S. aureus, B. Subtilis, Klebsiella, C. Coli* treated with the synthesized CuO and Zn-CuO NPs.

The results revealed that the appreciable antibacterial activity against *S. aureus, B. subtilis,*

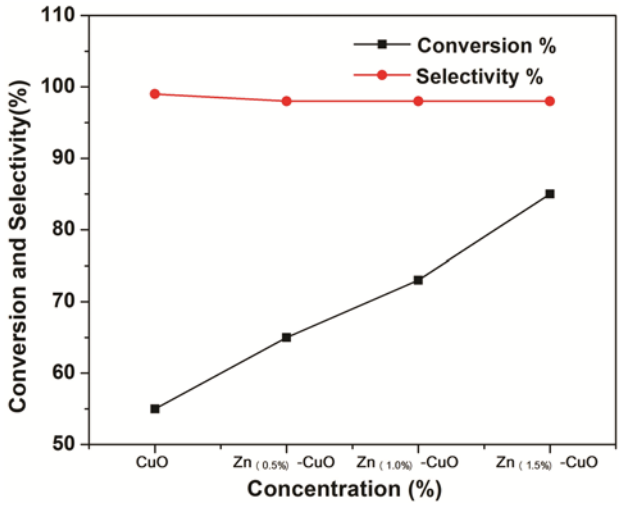

Fig. 5 — Catalytic activity of CuO by varying concentration of doped Zn.

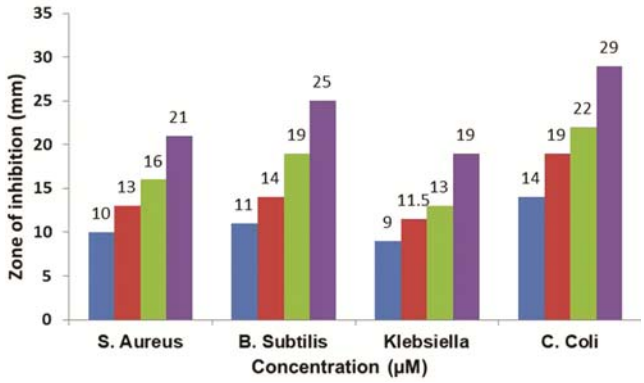

Fig. 6 — Antibacterial activity of CuO, and Zn-CuO NPs.

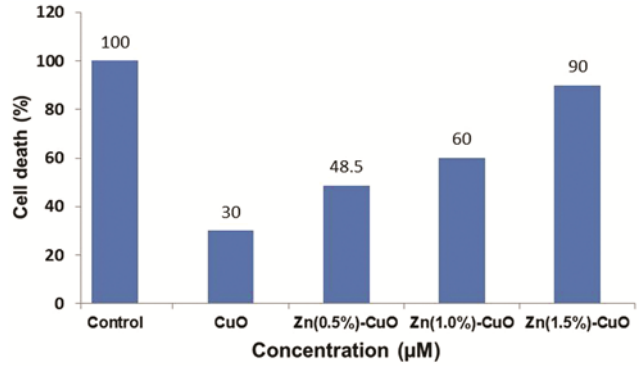

Fig. 7 — Cytotoxicity of CuO, and Zn-CuO NPs against A549 cancer cells.

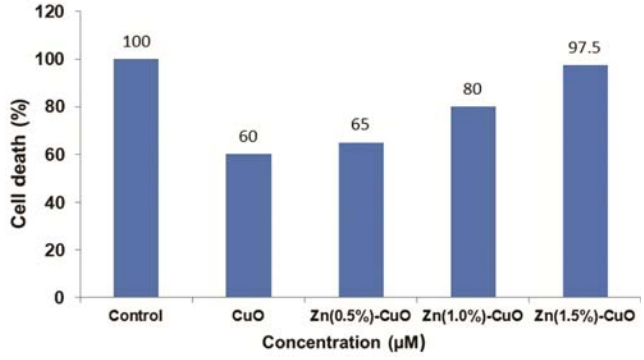

Fig. 8 — Cytotoxicity of CuO, and Zn-CuO NPs against MCF7 cancer cells.

Klebsiella, C. Coli. Figure 6 depicted that Zn-CuO with high dopant concentration showed maximum zone of inhibition against all the bacterial strains with the zone of inhibition ranging from 19-29 mm. The prominent inhibition was observed against *C. Coli* with maximum zone of inhibition of 29 mm with minimum inhibitory concentration (MIC) of 0.09 µM.

3.6 Antioxidant activity

The results of the antioxidant activity of CuO and various concentrations of Zn-CuO NPs were determined using percentage inhibition of DPPH and H_2O_2 free radicals oxidation (Table 1). When the stable DPPH radical accepts an electron from the antioxidant compound, the violet color of DPPH radical was reduced to yellow colored diphenylpicrylhydrazine radical. It was measured by colorimetric method. From the results it was inferred that material exhibited the antioxidant activity in the range of 18.99 ± 0.77% (CuO) to 65.54 ± 0.23% (Zn-CuO) by inhibiting the DPPH oxidation. It was also observed that H_2O_2 percentage inhibition increased with increasing concentration of the undoped CuO (Table 1). Zn-CuO NPs possessed significant and imperative antioxidant activity than that of undoped CuO NPs. The reason for this observation was Zn doping into CuO matrix may lead to formation of structural defects such as oxygen vacancies and Cu interstitial defects. These defects may act as trapping centres for electrons and it was expected to release more Cu^{2+} ions into the solution from interstitial sites as compared to that of undoped CuO[1].

Table 1 — Antioxidant activity of CuO and Zn-CuO NPs evaluated by DPPH and H_2O_2 free radical scavenging assay

Compounds	DPPH	H_2O_2
	Percentage of Inhibition	
CuO	18.99 ±0.77	21.56±0.96
$Zn_{(0.5\%)}$-CuO	21.90±0.85	18.76±0.76
$Zn_{(1.0\%)}$-CuO	35.32±0.96	29.34±0.98
$Zn_{(1.5\%)}$-CuO	65.54±0.23	59.12±0.12

3.7 Cytotoxic studies

The cytotoxic activity of the material was screened against human lung (A549) and human breast (MCF7) cell lines using MTT assay in a dose dependent fashion[40]. The graph of percentage of cell death and the concentration of the compounds under investigation were shown in the Figs 7 and 8. The results clearly indicated that the percentage of cell death of Zn-CuO NPs was higher than that of the undoped CuO NPs. Enhanced cytotoxicity was observed with the increase in the dopant concentration. Further, the synthesized Zn-CuO NPs exhibited better activity against MCF7 cell lines than A549 cell lines.

4 Conclusion

CuO and Zn-CuO NPs have been synthesized by microwave assisted method. The XRD analysis has been confirmed the monoclinic crystalline nature of Zn-CuO NPs and also revealed that the crystallite size

decreases from 30.43 to 19.24 nm on doping with increasing concentration of dopant. The structure of CuO (spheroid structure) and Zn doped CuO (nanorod structure) have been well differentiated using SEM analysis. BET analysis has been confirmed the particle size (30 nm) and surface area (46 m^2/g) of CuO. The particle size of Zn-CuO NPs was found to be 19 nm with increased surface area of 78 m^2/g. This results clearly indicated that the surface area of Zn doped CuO was higher than CuO. The results of antibacterial studies have been revealed that the Zn-CuO NPs showed maximum zone of inhibition against *C. Coli* (29 mm). Zn-CuO NPs have been exhibited strong antibacterial activity with minimum inhibitory concentration (MIC) of 0.09 µM. Further, Zn-CuO NPs have been shown significant cytotoxic activity against MCF7 cell lines than A549 cell lines. Finally, Zn dopant has been found to be very effective in enhancing the catalytic, antibacterial, antioxidant and cytotoxic potential of CuO NPs.

Acknowledgments

R. S thanks Dr. R. Karvembu, National Institute of Technology, Tiruchirappalli for providing the lab facilities.

References

1 Iqbal J, Jan T, Hassan S U L, Ahmed I, Mansoor I Q, Umair Ali M, Abbas F, & Ismail M, *AIP Advances*, 5 (2015) 127112.
2 Zhu J, & Qian X, *J Solid State Chem*, 183 (2010) 1632.
3 Chang Y N, Zhang M, Xia L, Zhang J, & Xing G, *Materials, 5* (2012) 2850.
4 Sathyamoorthy R, & Mageshwari K, *Physica E*, 47 (2013) 157.
5 Ighalo J O, Sagboye P A, Umenweke G, Ajala O J, Omoarukhe F O, Adeyanju C A, Ogunniyi S , & Adeniyi A G, *Environ Nanotechnol Monit Manag*, 15 (2021) 100443.
6 Rajput V, Minkina, T, Ahmed B, Sushkova S, Singh R, Soldatov M, Laratte B, Fedorenko A, Mandzhieva S, & Blicharska E, *Rev Environ Contam Toxicol*, 252 (2019) 51.
7 Qin H, Zhang Z, Liu X, Zhang Y, & Hu J, *J Magn Magn Mater*, 322 (2010) 1994.
8 Cheng Z, Xu J, Zhong H, Chu X , & Song J, *Mater Lett*, 65 (2011) 2047.
9 Aslani A, & Oroojpour V, *Physica B*, 406 (2011) 144.
10 Wijesundera R P, *Semicond Sci Technol,* 25 (2010) 045015.
11 Jan T, Iqbal J, Ismail M, Badshah N, Mansoor Q, Arshad A, & Ahkam Q M, *Mat Sci Semicon Proc*, 21 (2014) 154.
12 Kumar A, Kuang Y, Liang Z, & Sun X, *Mater. Today Nano*, 11 (2020) 100076.
13 Kannan K, Radhika D, Vijayalakshmi S, Sadasivuni K K, Adaeze A Ojiaku, & Verma U, *Int J Environ Anal Chem*, (2020) 1.
14 Subramanian B, Priya K, Rajan A, Dhandapani S T, & Jayachandran M, *Mater Lett*, 128 (2014) 1.
15 Nahhal I, Zourab M E L, Kodeh S M, Selmane F S, Genois M, & Babonneau F, *Int Nano Lett*, 2 (2012) 1.
16 Thakur N, Anu, Kumar K, & Kumar A, *Dalton Trans*, 50 (2021) 6188.
17 Jayaprakash J, Srinivasan N, Chandrasekaran P, & Girija E K, *Spectrochim Acta, Part A*, 136 (2015) 1803.
18 Saranya R, & Mubarak Ali M, *Acta Chim Slov*, 67 (2020) 235.
19 A Khalid A, Ahmad P, Alharthi A I, Muhammad S, Khandaker M U, Rehman M, Faruque M R I, Din I U, Alotaibi M A, Alzimami K, & Bradley D A, *Nanomaterials*, 11 (2021) 451.
20 Jan T, Iqbal J, Mansoor Q, Ismail M, Naqvi SH, Gul A, Naqvi S F H , & Abbas F, *J Phys D Appl. Phys*, 47 (2014) 355301.
21 Malka E, Perelshtein I, Lipovsky A, Shalom Y, Naparstek L, Perkas N, & Gedanken A, *Small*, 9 (2013) 4069.
22 Xiao L, Huanli X, Cong L, Gan Q, Ammad A F, Aharon G, Xiaohui L, & Xiukun L, *Front Pharmacol*, 10 (2019) 1.
23 Xue Y, Yu G, Shan Z, & Li Z, *J Photochem Photobiol B*, 186 (2018) 131.
24 Mishra R K, Kumar V B, Victor A, Pulidindi A L, & Gedanken A, *Ultrason Sonochem*, 56 (2019) 55.
25 Ashraf R, Bashir M, Raza M A, Riaz S, & Naseem S, *IEEE Trans Magn*, 51 (2015) 1.
26 Sanjini N S, & Velmathi S, *J Porous Mater*, 23 (2016) 1527.
27 Muthuvel A, Jothibas M , & Manoharan C, *Nanotechnol Environ Eng*, 5(14) (2020) 32.
28 Das D, Nath B C, Phukon P, Kalita A, & Dolui S K , *Colloid Surf B*, 111 (2013) 556.
29 Muthuvel A, Jothibas M, Manoharan C, & Jayakumar S J, *Res Chem Intermediat*, 46 (2020) 2705.
30 Loganayaki N, Siddhuraju P, & Manian S, *Food Sci Tech,* 50 (2011) 687.
31 Kumar R S, Rajkapoor B, & Perumal P, *Asian Pac J Trop Biomed*, 2 (2012) 256.
32 Kumar P, Mathpal M C, Prakash J, Viljoen B C, Roos W D, & Swart H C, *J Alloys Compd* 832 (2020) 154968.
33 Cakmak H M, Cetinkara H A, & Kahraman S, *Superlattices Microstruct*, 51 (2012) 421.
34 Niasari M S, Davar F, & Khansari A, *J Alloy Compd*, 509 (2011) 61.
35 Basith N M, Vijaya J J, Kennedy L J, & Bououdina M, *Physica E*, 53 (2013) 193.
36 Raza M A, Kanwal Z, Rauf A, Sabri A N, Riaz S, & Naseem S, *Nanomaterials*, 6(4) (2016) 74.
37 Solanki P R, Kaushik A, Agrawal V V , & Malhotra B D, *NPG Asia Materials*, 3 (2011) 17.
38 Mishra R K, Kumar V B, Victor A, Pulidindi I N, & Gedanken A, *Ultrason Sonochemistry*, 56 (2019) 55.
39 Hong X, Wen J, Xiong X, & Hu Y, *Environ Sci Pollut Res*, 23 (2016) 4489.
40 Kuppusamy P, Ichwan S J A, Al-Zikri P N H, Suriyah W H, Soundharrajan I, Govindan N, Gaanty P M, & Mashitah M Y, *Biol Trace Elem Res*, 173 (2016) 297.